# DRAG OF THE SEA SURFACE

V. K. MAKIN, V. N. KUDRYAVTSEV* and C. MASTENBROEK**
*Royal Netherlands Meteorological Institute (KNMI), De Bilt, The Netherlands*

(Received in final form 9 September, 1994)

**Abstract.** It is shown how the drag of the sea surface can be computed from the wind speed and the sea state. The approach, applicable both for fully developed and for developing seas, is based on conservation of momentum in the boundary layer above the sea, which allows one to relate the drag to the properties of the momentum exchange between the sea waves and the atmosphere.

The total stress is split into two parts: a turbulent part and a wave-induced part. The former is parameterized in terms of mixing-length theory. The latter is calculated by integration of the wave-induced stress over all wave numbers. Usually, the effective roughness is given in terms of the empirical Charnock relation. Here, it is shown how this relation can be derived from the dynamical balance between turbulent and wave-induced stress. To this end, the non-slip boundary condition is assigned to the wave surface, and the local roughness parameter is determined by the scale of the molecular sublayer.

The formation of the sea drag is then described for fully developed and developing seas and for light to high winds.

For the Charnock constant, a value of about $0.018 - 0.030$ is obtained, depending on the wind input, which is well within the range of experimental data.

It is shown that gravity-capillary waves with a wavelength less than 5 cm play a minor role in the momentum transfer from wind to waves. Most of the momentum is transferred to decimeter and meter waves, so that the drag of developing seas depends crucially on the form of the wave spectrum in the corresponding high wavenumber range.

The dependence of the drag on wave age depends sensitively on the dependence of this high wavenumber tail on wave age. If the tail is wave-age independent, the sea drag appears to be virtually independent of wave age. If the tail depends on wave age, the drag also does. There is contradictory evidence as to the actual dependence. Therefore, additional experiments are needed.

## 1. Introduction

Estimation of the surface flux of momentum above the sea and its dependence on sea state is a challenging problem of air-sea interactions with several important applications, such as climate research and remote sensing.

The bulk aerodynamic formulation (e.g. Geernaert, 1990) connects the momentum flux at the surface $\tau$ to the mean wind speed at some reference level (usually at 10 m) $U_{10}$ via the drag coefficient $C_d$:

$$\tau = \rho_a C_d U_{10}^2, \tag{1}$$

where $\rho_a$ is air density. Assuming a logarithmic velocity profile

$$u(z) = \frac{u_*}{\kappa} \ln \frac{z}{z_0}, \tag{2}$$

* On leave from Marine Hydrophysical Institute, Sevastopol, Crimea

** The investigation was in part supported by the Netherlands Geosciences Foundation (GOA) with financial aid from the Netherlands Organization for Scientific Research (NWO).

*Boundary-Layer Meteorology* **73:** 159–182, 1995.

where $u_* = \sqrt{\tau/\rho_a}$ is the friction velocity, $\kappa$ is the von Karman constant and $z_0$ is the roughness parameter. The drag coefficient $C_d$ at 10 m height is expressed as

$$C_d = \frac{\kappa^2}{\ln^2(10/z_0)}. \tag{3}$$

For winds below 3 m/s, the sea is calm, with few or no waves present. The air flow above the sea corresponds to that over an aerodynamically smooth surface (Phillips, 1977; Geernaert, 1990), and the roughness parameter is determined by the scale of the molecular sublayer (Monin and Yaglom, 1971):

$$z_0 = c_1 \frac{\nu}{u_*}, \tag{4}$$

where $\nu$ is the air viscosity and $c_1$ is a constant of $O(10^{-1})$.

With wind increasing, waves begin to grow and to extract momentum from the air. In the limit of high winds, the sea surface can be described as aerodynamically rough. The roughness parameter depends on the mean square surface displacement of the short gravity waves, which in turn is determined by the friction velocity and acceleration of gravity $g$ (Phillips, 1977):

$$z_0 = c_h \frac{u_*^2}{g}. \tag{5}$$

Eq.(5) is known as the Charnock relation, as it was originally obtained on dimensional reasoning by Charnock (1955). The Charnock parameter $c_h$ is usually assumed to be a constant. Based on measurements, different values for $c_h$ have been suggested, ranging from 0.014 (Garratt, 1977) to 0.018 (Wu, 1980) and 0.035 (Kitaigorodskii, 1970).

After the roughness parameter is defined, equations (2), (3), (5) can be solved iteratively to obtain the drag coefficient for a given wind speed $U_{10}$, and the stress on the sea surface can be estimated from (1). Taking $c_h = 0.014$ in (5) the following relation is obtained by Garratt (1977):

$$C_d = (0.75 + 0.067U_{10})10^{-3}. \tag{6}$$

Relation (6) applies in the range of the wind speed $5 < U_{10} < 20$ m/s. Numerous parameterizations of the drag coefficient in the form of (6), based on the experimental data, are compiled in Geernaert (1990).

The Charnock relation suggests that the sea drag is determined by the wind. In coastal regions and in atmospheric synoptic frontal zones, the sea state varies rapidly in space and time. Here one may expect the momentum flux to depend both on the wind speed and the sea state. In principle, the state of the sea is characterized by the wave spectrum $S(\omega)$. But often detailed spectral information is lacking. For a pure wind sea, attempts have been made to characterize the sea state in terms of one parameter, the inverse wave age, $\tilde{\Omega} = U_{10}/c_p$ (or $u_*/c_p$), where $c_p$ is the

phase speed of the component in the peak of the spectrum. For a fully developed sea, $\tilde{\Omega} = 0.83$, for a mature one, $\tilde{\Omega} \sim 1.5$, and for young seas, $\tilde{\Omega} \sim 2 - 3$.

To account for a possible wave-age dependence of the sea drag, the Charnock parameter is often assumed to be a power function of the wave age:

$$z_0 \frac{g}{u_*^2} = \chi \left( \frac{u_*}{c_p} \right)^m , \tag{7}$$

where the parameters $\chi$ and $m$ can in principle be estimated experimentally. The relation (7) gives an increase of $z_0$ and the drag coefficient for young seas if $m$ is positive.

In Smith *et al.* (1992), relation (7) was fitted to HEXOS experimental data, resulting in values of $m \sim 1$ and $\chi = 0.48$. However, it was found (Smith *et al.*, 1992, pg.134), that "variation of $c_p/u_*$ is due more to $u_*$ than to $c_p$ and self-correlation has influenced the fit to obtain equation (7)" (with $m \sim 1$ and $\chi = 0.48$). This fact does not disprove, but on the other hand does not establish relation (7).

Toba *et al.* (1990) combined field and laboratory data to argue an opposite trend in (7), estimating parameter $m$ to be negative: $m = -1$. Donelan *et al.* (1993), disregarding laboratory data, accepted the parameters of Smith *et al.* (1992).

Recently, a new approach to describe the drag of the sea surface and to account for developing seas was suggested by Janssen (1989, 1991, 1992) and Chalikov and Makin (1991). Their models differ in details, but are conceptually the same (Mastenbroek et al., 1993). The approach is based on the conservation of momentum in the boundary layer above the sea, which implies that the stress is independent of height, so that the momentum flux at a given height is equal to the momentum flux into the sea. The drag of the sea surface results from a dynamical balance of the turbulent and wave-induced stresses. The momentum flux above the sea is split into two parts: a turbulent stress and a wave-induced stress. The former is parameterized in terms of mixing-length theory. To calculate the surface turbulent stress, a "background" roughness parameter is defined via Charnock-type relations. For seas which are close to fully developed, the Charnock-type relations ensure that proper values of the drag coefficient are used.

The total wave-induced stress is then calculated by integration of the wave-induced stress going into individual wave components, up to a certain wavenumber. The result depends on the wave spectrum in the wavenumber range considered and on the assumed growth rates of the individual wave components. Once the turbulent and wave induced stress are known, the drag coefficient follows.

The wave age dependence of the drag coefficient results from the wave age dependence of the wave stress and from assumptions concerning the background roughness parameter. Calculations of Janssen (1989), Chalikov and Makin (1991) and Chalikov and Belevich (1993) show that for high winds, the drag coefficient is more than twice as large for young seas as it is for old ones. However, in their

approach the result is sensitive to the assumed background roughness, which is not accessible to computation.

Caudal (1993) bypassed this problem by considering the situation in which all stress is supported by waves. Using a logarithmic profile for the wind velocity and wave spectra of Donelan and Pierson (1987) and Donelan *et al.* (1985), he could derive the Charnock relation as a result of consistency between the surface stress, wind input and spectral shape. The resulting Charnock constant of 0.012 has the correct magnitude, which illustrates the usefulness of Caudal's approach. It is however valid only for high winds and a fully developed wind sea.

We present here a generalized approach, which is valid for fully developed and developing seas and for light to high winds. The general idea is still based on conservation of momentum in the boundary layer above the sea. But to avoid parameterization of the background roughness, we shall make two principal assumptions. First, all undulations of the sea surface are regarded as waves. The assumption allows the statistical description of sea waves in terms of a wave spectrum in the full wave-number range, and presupposes that the wave growth parameter can be defined for the full wave-number range (the same assumption was made in Janssen (1989) and Caudal (1993)). The validity of this assumption could be limited at the very short length scales, when foam or non-wave-like surface deformations appears on the surface.

As soon as this assumption is accepted and the sea surface is treated as a superposition of waves to the smallest scales, the second assumption follows: a non-slip molecular viscosity boundary condition on the instantaneous wave surface. This allows the use of the viscous roughness as roughness parameter, which is universal for all sea states.

Once these assumptions have been made, one may give a consistent description of the momentum flux above fully developed and young seas, and the effective roughness (defined as the constant in the logarithmic wind profile obtained sufficiently far above the waves) can be derived as a result of the dynamical balance of the turbulent and wave-induced stresses. This roughness turns out to be proportional to the friction velocity squared, so the Charnock relation (5) is derived. As a result, the drag coefficient increases with wind speed. It turns out that most of the drag is supported by short gravity waves. For light winds ($U_{10} < 5$ m/s) the stress at the surface is dominated by the viscous drag.

For a wind sea one may study the wave-age dependence of the drag coefficient, for a given wind speed. This obviously depends on the wave-age dependence of the wave spectrum. When we assume that the wave spectra of Donelan and Pierson (1987) and Donelan *et al.* (1985) apply to all wave ages, we obtain a drag that is virtually independent of the wave age. This is a consequence of the fact that the wave-induced flux to the high frequency tail of the wave spectrum is wave-age independent. However, if a weak wave-age dependence is introduced in the description of the tail, the sea drag becomes wave-age dependent. There is contradictory evidence as to the actual dependence.

## 2. The structure of the momentum flux above waves

We consider the lower part of the atmospheric boundary layer above the sea, the structure of which crucially depends on the sea state. We call this part of the boundary layer the "wave boundary layer " or the WBL. At the upper boundary of the WBL, the wave-induced momentum flux is negligible. The wave-induced velocities of the wave component with a wave number $k$ decay on scale $z \sim k^{-1} \sim c^2/g$. For a fully developed sea, the phase speed of the component of the peak of a wave spectrum is $c \sim U_{10}$. Thus for a wind speed of 10 m/s, the decay scale is 10 m. The wave-induced momentum flux which above waves is quadratic in wave-induced quantities, decays much faster. That suggests that a height $h$ of 10 m is a good estimate of the upper boundary of the WBL.

The adjustment time of a turbulent boundary layer is determined by its characteristic height $h$ and the friction velocity $u_*$, $T_a \sim h/u_*$. For $h \sim 10$ m and $u_* \sim 0.25$ m/s, we obtain $T_a \sim 40$ s. The evolution time scale of the sea waves is a few hours and is much longer than $T_a$. That means that WBL can be treated as stationary.

Assume a wind blowing in the positive X direction independent of the horizontal spatial coordinates. Under steady conditions:

$$\frac{\partial \hat{\tau}}{\partial \hat{z}} = 0 \tag{8}$$

and the momentum flux, normalized on the density of the air $\hat{\tau}$, is constant over height:

$$\hat{\tau} = \frac{\tau}{\rho_a} = \text{Const.} = u_*^2. \tag{9}$$

$\hat{z}$ is a vertical coordinate

$$\hat{z} = h\frac{z - \eta}{h - \eta}, \tag{10}$$

which follows the wave surface $z = \eta$ ( $\hat{z} = 0$). Hereafter we drop the top hat $\hat{}$ over $z$ and $\tau$.

The momentum flux $\tau$ can be split into a part supported by turbulence $\tau^t$, a viscous stress $\tau^\nu$ and a wave-induced part $\tau^w$ (Janssen, 1989; Makin, 1990):

$$u_*^2 \equiv \tau = \tau^t(z) + \tau^\nu(z) + \tau^w(z). \tag{11}$$

At the upper boundary of the WBL, $\tau^w(h) = \tau^\nu(h) = 0$ and the total flux is supported only by the turbulent stress $\tau^t(h) = \tau$. At the water surface $\tau^t(0) = 0$ and the total flux is supported by the viscous stress and the wave-induced stress.

A mixing-length model is used to parameterize the turbulent stress

$$\tau^t(z) = K\frac{\mathrm{d}u}{\mathrm{d}z} = l^2\frac{\mathrm{d}u}{\mathrm{d}z}\left|\frac{\mathrm{d}u}{\mathrm{d}z}\right|, \tag{12}$$

where $K$ is the eddy viscosity coefficient, and $l = \kappa z$ is the turbulent mixing length.

The viscous stress is

$$\tau^{\nu}(z) = \nu \frac{d^2 u}{\mathrm{d}z^2}. \tag{13}$$

We consider all undulations of the sea surface as waves, which can then be statistically described by a directional wave spectrum $S(k, \theta)$, where the wave number $k$ satisfies the dispersion relation

$$\omega^2 = gk + Tk^3, \tag{14}$$

where $T$ is the dynamical surface water tension and $\theta$ is the propagation direction of the $k$-wave component. We assume that the energy input to the waves from the atmosphere is known and can be described in terms of the growth rate parameter $\beta(k, \theta)$. Both $S$ and $\beta$ are wind dependent.

The wave-induced stress to the $k$ component of a wave spectrum (integrated over directions) at the surface is (e.g., Phillips, 1977)

$$M(k) = \int_{-\pi}^{\pi} \omega^2 S \beta \cos\theta \, k \, \mathrm{d}\theta. \tag{15}$$

The wave-induced stress to all waves is

$$\tau_0^w = \int_0^{\infty} M(k) \, \mathrm{d}k. \tag{16}$$

Numerical calculations of Makin (1989), presented by Chalikov and Belevich (1993) in their Figure 3, show that for the given wavenumber $k$, the wave-induced stress decays with height $z$ according to approximately $\exp(-2kz)$. The vertical distribution of the wave-induced stress flux can then be written:

$$\tau^w(z) = \int_0^{\infty} M(k) e^{-2kz} \, \mathrm{d}k. \tag{17}$$

The set of equations (11), (12), (17) requires two boundary conditions:

$$z = 0 : u = 0 \tag{18}$$

and

$$z = h : u = U_{10}. \tag{19}$$

To avoid the explicit description of the flow within the viscous sublayer, of which the height $\delta_\nu \sim \nu / u_*^l$ is relative to the instantaneous wave surface $z = 0$, we use the standard matching of the linear and logarithmic profiles (e.g., Monin and Yaglom, 1971) within $\delta_\nu$. The friction velocity at the top of the molecular sublayer $u_*^l$ should be taken as

$$u_*^l = \sqrt{u_*^2 - \tau_0^w} \tag{20}$$

due to (11), because at heights $z > \delta_\nu$ the viscous stress $\tau^\nu$ can be neglected.

The surface boundary condition (18) can now be rewritten

$$z = z_0 : u = 0, \tag{21}$$

where the roughness parameter $z_0$ is

$$z_0 = 0.14\frac{\nu}{u_*^l}, \tag{22}$$

and the term $\tau^\nu$ in (11) can be dropped. It is possible to rewrite the boundary condition and to define the roughness parameter because that very short waves with lengths $\lambda \leq \delta_\nu$ do not contribute to the wave-induced stress $\tau^w$, or, in other words, that the wave-induced stress $\tau^w$ is constant within $\delta_\nu$. This condition is satisfied by the choice of the wave spectrum and $\beta$ parameter (section 2.1).

The dynamical roughness of the sea surface (defined as the constant in the logarithmic wind profile obtained sufficiently far above the waves) can be derived as a result of the dynamical balance of the turbulent and wave-induced stresses.

The wind profile and the friction velocity $u_*$ follow from the solution of the model in the domain $z_0 \leq z \leq h$.

## 2.1. Wave-induced flux at the surface

At this point it becomes clear that results of the present approach will depend on the model of a wave spectrum $S$ and on the choice of the growth rate parameter $\beta$. To proceed, we have to make choices.

### 2.1.1. *Wave spectrum*

Recently there has been an extensive discussions on the form of a wave spectrum by Banner *et al.* (1989), Banner (1990), Battjes *et al.* (1987), Donelan *et al.* (1985), Donelan and Pierson (1987) and Kitaigorodskii (1992). Following these discussions, we use a parameterization suggested by Donelan *et al.* (1985) for the energy-containing part of the spectrum $0 < k/k_p < 10k_p^0$:

$$S(k,\theta) = \frac{1}{2}\alpha_p k^{-4}\sqrt{k/k_p}\exp(-(k_p/k)^2)\gamma^\Gamma f_{h_1,\theta}, \tag{23}$$

$$\alpha_p = 0.006\tilde{\Omega}^{0.55}, \tag{24}$$

$$\gamma = 1.7 + 6\log(\tilde{\Omega}), \tag{25}$$

$$\Gamma = \exp(-(\sqrt{k/k_p} - 1)^2/2\sigma^2), \tag{26}$$

$$\sigma = 0.08(1 + 4\tilde{\Omega}^{-3}), \tag{27}$$

where $0.83 < \tilde{\Omega} = U_{10}/c_p < 5$ and the angular spreading function $f_{h_1,\theta}$ is given by

$$f_{h_1,\theta} = \frac{1}{2}h_1\cosh^{-2}(h_1\theta) \tag{28}$$

$$\overline{\eta^2} = \int_0^\infty \int_{-\pi}^{\pi} S(k,\theta)\, k\, dk\, d\theta$$

with

$$h_1 = 1.24, \quad \text{if} \quad 0 < k/k_p < 0.31 \tag{29}$$

$$h_1 = 2.61(k/k_p)^{0.65}, \quad \text{if} \quad 0.31 < k/k_p < 0.90 \tag{30}$$

$$h_1 = 2.28(k/k_p)^{-0.65}, \quad \text{if} \quad 0.90 < k/k_p < 10. \tag{31}$$

The wave number of the peak of the spectrum $k_p = g/c_p^2 = g(\tilde{\Omega}/U_{10})^2$ and the peak wave number $k_p^0$ of a fully developed sea $\tilde{\Omega} = 0.83$ are

$$k_p^0 = \frac{g}{(1.2U_{10})^2}. \tag{32}$$

A dependence of the spectral level of the energy-containing part of the spectrum (23) on wave age ($\sim \tilde{\Omega}^{0.55}$) has been found in several studies (Banner, 1990; Battjes *et al.*, 1987; JONSWAP group, 1971).

The form of the high wave number spectrum $k \geq 10k_p^0$ is from Donelan and Pierson (1987). The main feature of this spectrum is that it contains no dependence on wave age.

Radar backscatter measurements of the sea surface provide an accurate estimate of the two-dimensional wave spectrum for high frequency waves (see Donelan and Pierson, 1987). Donelan and Pierson use these data to construct a form of the wave spectrum for high wave numbers. The form of the high wave number equilibrium spectrum was derived on the assumption that it results from a balance between direct wind forcing and dissipation due to breaking and to viscosity:

$$S(k,\theta) = k^{-4}\left(\frac{2.510^{-4}}{\alpha}\left(\frac{u(\lambda/2)}{c} - 1\right)^2 - \frac{4\nu_w k}{c\alpha}\right)^{1/n} 2h_1^{-1} f_{h_1,\theta}, \tag{33}$$

where $\nu_w$ is the water viscosity and the angular spreading parameter $h_1$ is

$$h_1 = \frac{0.46}{\sqrt{2(1 - 0.8^{n/2})}}. \tag{34}$$

The coefficients $n(k)$ and $\alpha(k)$ were then found by fitting the spectral level to observations obtained by backscatter measurements. Expressions for $n$ and $\alpha$ can be found in Donelan and Pierson (1987).

The spectrum (33) has a cut-off at a wave number where the input from the wind is equal to viscous dissipation. The functional relation (34) deteriorates in the vicinity of the cut-off, but we shall show that the concrete form of the spectrum near the cut-off plays an insignificant role in supporting the sea drag. The cut-off in the gravity-capillary range is confirmed by radar backscatter measurements in Ku-band (Donelan and Pierson, 1987). Jähne and Riemer (1990) analysed the slope frequency spectra and reported a cut-off frequency at wave numbers between $430 - 1020\ \mathrm{m}^{-1}$, which does not contradict Donelan and Pierson (1987). However,

they argue that the cut-off is not the result of the balance between wind input and viscous dissipation.

With a typical value of the thickness of the viscous sublayer $\delta_\nu \sim 10^{-4}$ m and cut-off wavelength of $6 \cdot 10^{-3}$ m, the condition that waves shorter than $\lambda \leq \delta_\nu$ do not contribute to the wave-induced stress is satisfied.

Spectra (33) and (23) can be patched by the relation

$$k_r = 10k_p^0(1.2U_{10}/c_p)^{3/2}, \tag{35}$$

which follows from equating spectral levels of the spectra (33) and (23), integrated over direction.

The wave spectrum is now defined in the full wave-number range. The spectrum (23) is associated with the energy-containing waves ($k < k_r$) and (33) with high wave-number waves ($k > k_r$).

This model of the wave spectrum was originally suggested by Donelan and Pierson (1987) for a fully developed sea with $U_{10}/c_p = 0.83$. Extension of the model to developing seas is our assumption, which does not contradict the present experimental evidence on the wave spectral form.

Recent reanalysis of the original data of the JONSWAP experiment was performed by Battjes *et al.* (1987). No dependence of the high frequency part ($1.5f_p < f < 1Hz$) of the wave spectrum on the stage of wave development (in terms of $\tilde{\Omega}$) is found.

Reliable measurements of the directional wave spectrum were performed by Banner *et al.* (1989). Their analysis shows no wave-age dependence in the range of wavelength 0.2–1.6 m. However, their analysis is valid only in the range of wind speed 7 m/s $< U_{10} <$ 13 m/s and inverse wave age $\tilde{\Omega} \sim 0.8 - 1.6$, and more data are needed to establish whether the high wave spectrum is wave-age dependent or not (private communication, Banner).

Kitaigorodskii (1992) has analysed a number of experiments to conclude that in the high wave-number range $k/k_p > 9 - 25$, the Phillips parameter in the $\omega^{-5}$ spectrum $\alpha_p$ is virtually a constant.

The wave-age dependence of the high wave-number spectrum is a controversial question. That is why, in order to reveal the consequences of the wave spectrum model on the solution of the problem, we performed the following experiment. The wave spectrum (33) was allowed to depend on the inverse wave-age parameter as $\tilde{\Omega}^{2/5}$, while the energy-containing part (23) and the patching wave number $k_r$ were kept the same.

To reveal the impact of the energy-containing part, we took the JONSWAP form of the wave spectrum instead of (23). The Phillips parameter $\alpha_p$ was taken to be wave-age dependent, as suggested by Snyder (1974) and used in the models of Janssen (1989), Chalikov and Makin (1991) and Chalikov and Belevich (1993):

$$\alpha_p = 0.57(\tilde{\Omega})^{3/2}. \tag{36}$$

This is a stronger dependence on $\tilde{\Omega}$ than was originally suggested by the JONSWAP Group (1971), $\sim \tilde{\Omega}^{2/3}$. The high wave-number part of the spectrum (33) and the patching wave number were kept the same.

2.1.2. *Wave growth-rate parameter*

The wind-wave interaction parameter or the wave growth rate parameter $\beta$ is defined as

$$\beta_\rho = \frac{\rho_a}{\rho_w}\beta = \frac{1}{\omega S}\frac{\partial S}{\partial t}. \tag{37}$$

The well-known parameterizations of $\beta$ based on field experimental data are by Snyder *et al.* (1981):

$$\beta = 0.25(\mu_5 - 1), \tag{38}$$

where $1 < \mu_5 = U_5/c < 4$ ($U_5$ is a wind at 5 m height) and by Hsiao and Shemdin (1983):

$$\beta = 0.12(\mu_{10} - 1)^2, \tag{39}$$

where $1 < \mu_{10} = 0.85U_{10}/c < 7.4$. Measured growth rates in Hasselmann and Bösenberg (1991) are reported to be in agreement with Snyder *et al.* (1981).

Donelan and Pierson (1987) made a reanalysis of the experimental laboratory data of Larson and Wright (1975) for short waves ($100 < k < 900$) and suggested

$$\beta = 0.072(\mu_{\lambda/2} - 1)^{2.33}, \tag{40}$$

where $\mu_{\lambda/2} = u_{\lambda/2}/c$.

Plant (1982) has shown that $\beta$ values from several laboratory and field experiments are quadratically dependent on $\mu_* = u_*/c$

$$\beta = \frac{\rho_w}{\rho_a}0.04\mu_*^2, \tag{41}$$

where $0.05 < \mu_* < 3$.

Dimensional analysis of the Reynolds equations describing the interaction of the turbulent air flow with waves shows that $\beta$ should be a function not only of the wave age $U/c$ (or $u_*/c$) but also of the drag coefficient $C_d = (u_*/U)^2$, if a relation between $u_*$ and $U$ is not specified *a priori* (Burgers and Makin, 1993). Numerical calculations of Burgers and Makin (1993) have shown that the growth-rate parameter indeed depends on both: the wave-age parameter $\mu_\lambda = u_\lambda/c$ and the drag coefficient $c_\lambda = u_*^2/u_\lambda^2$. The friction velocity and wind speed are both related to the height $\lambda$.

Burgers and Makin (1993) have shown that calculations of $\beta$ can be well parameterized by the functional relation suggested by Stewart (1974), who proposed it on general theoretical considerations and some experimental knowledge:

$$\beta = a_1\frac{u_*}{c}(\mu_\lambda - a_2), \tag{42}$$

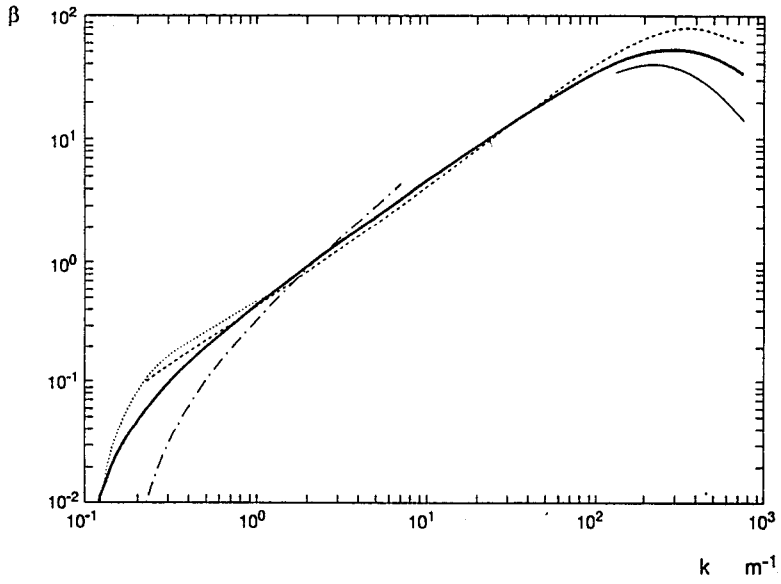


Fig. 1. The growth rate parameter $\beta$ as a function of wave number $k$. Wind speed $U_{10} = 10$ m/s. Dotted line - Snyder *et al.* (1981), eq.(38); dashed-dotted - Hsiao and Shemdin (1983), eq.(39); dashed - Plant (1982), eq.(41); thin solid - Larson and Wright (1975), eq.(40); thick solid - Stewart (1974), eq.(42) with $a_1 = 2.0$, $a_2 = 1.15$. Horizontal axis - $m^{-1}$.

$(a_1 = 1.2, a_2 = 1)$, which also includes dependence on both parameters.

Relationship (42) is a convenient compromise between the parameterizations of $\beta$ based on experimental data (Snyder, *et al.* 1981; Hsiao and Shemdin, 1983; Plant, 1982; and Larson and Wright, 1975) in the full wave-number range, if we take $a_1 = 2, a_2 = 1.15$. Parameterizations of $\beta$ are shown in Figure 1, where the X-axis represents wave numbers $k$ in 1/m. The growth rates are calculated for a given wind speed $U_{10} = 10$ m/s. To calculate friction velocity and velocities at different levels, relation (6) is used. We shall use parameterization (42) of $\beta$ in the present study.

Parameterization (42) has a plausible feature: it quenches the growth rates for short waves. As the waves get shorter towards the end of the spectrum, the wind speed used in their growth rate drops. In the capillary range, $\beta$ according to (42) is additionally quenched due to the increase of phase velocity with increasing wave number. This quenching mechanism is absent if the parameterization of Plant (41) is used, as was already noted by Caudal (1993).

In principle, the friction velocity in (42) should be determined by the local structure of turbulence, i.e., at height $\lambda$ : $u_*(\lambda) = \sqrt{u_*^2 - \tau^w(\lambda)}$, which provides a further quenching of the short waves. As $\tau^w$ drops very fast with height due to (17) (a few centimetres), only very short waves can be affected.

The quenching of the wave-induced stress $\tau_0^w$ at high wave numbers depends thus only marginally on the cut-off wavenumber of the spectrum (33).

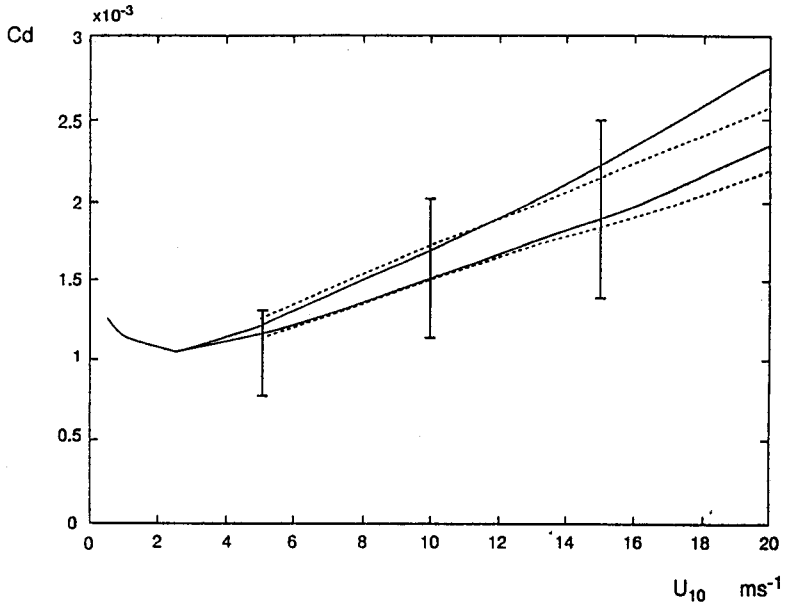


Fig. 2. Drag coefficient $C_d$ for fully developed sea $U_{10}/c_p = 0.83$ as a function of wind speed $U_{10}$ in m/s. Solid lines are model results (upper: $a_1 = 2.0$, lower: $a_1 = 1.6$ in eq.(42)). Dashed lines correspond to the Charnock relation (upper: $c_h = 0.03$, lower: $c_h = 0.018$ in eq.(5)). Vertical bars show the variability of $C_d$ parameterizations based on experimental data according to Geernaert (1990).

## 3. Results

To start a solution, the wind profile and the friction velocity are initialized by (2) and (5) for a given wind speed $U_{10}$ (in principle both the wind profile and the friction velocity can be initialized arbitrarily). The wave spectral density is then calculated with (23) and (33), using the patching relation (35). The wind input is calculated (42) and the wave-induced stress then follows from (15), (16) and (17). From (20) and (22), the roughness parameter is estimated and from (12) the turbulent stress is determined. Equation (11) is then solved with boundary conditions (19) and (21). Iterations continue until the total stress $\tau$ is constant within 1% over height.

The sea drag $C_d$ is thus found as a function of wind speed $U_{10}$ and the inverse wave-age parameter $\tilde{\Omega} = U_{10}/c_p$.

The drag coefficient for fully developed sea $\tilde{\Omega} = 0.83$ is shown in Figure 2. To assess the sensitivity of the model on the wind input, we use two values of the $a_1$ parameter in the parameterization (42) of $\beta$ , namely $a_1 = 2$ and $a_1 = 1.6$. The range of variability in the parameterizations of $C_d$ (see Table 2 in the review of Geernaert, 1990), based on field measurements, is shown by vertical bars in Figure 2. A bar is not shown for wind speeds of 20 m/s as there exist hardly any measurement for conditions of fully developed sea.

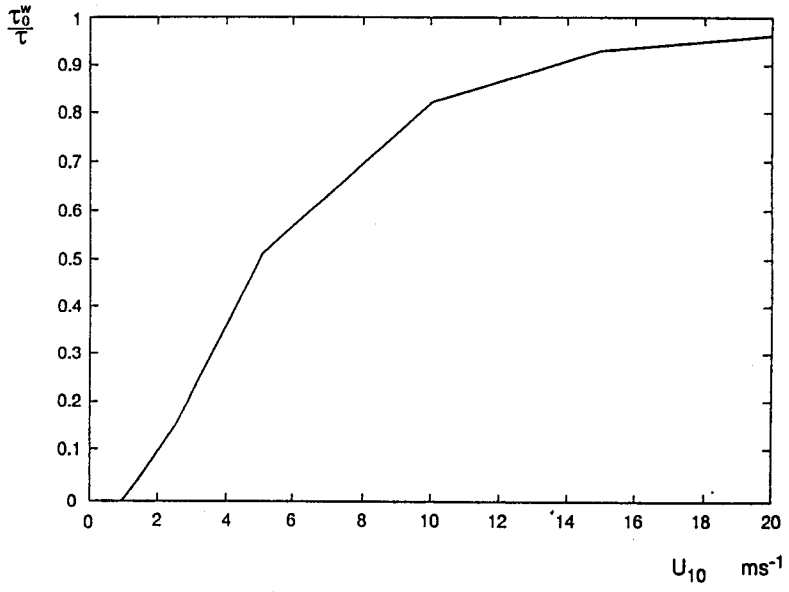


Fig. 3. Coupling parameter $\tau_0^w / u_*^2$ for a fully developed sea as a function of wind speed $U_{10}$.

For winds less than 2.5 m/s, the sea drag increases with decrease of wind speed indicating that the sea surface is aerodynamically smooth. For winds higher than 2.5 m/s, the sea drag increases with wind speed. Model results closely follow the drag coefficient resulting from the Charnock relation with $c_h = 0.018$ and $c_h = 0.03$. That means that with an increase of wind speed, the sea surface becomes rough. The values of the drag coefficient, which are plotted in Figure 2, lie well within the scatter of experimental data. Thus we have obtained the Charnock relation for the effective sea roughness as a solution of the model.

Figure 3 shows the coupling parameter $\tau_0^w / u_*^2$ for fully developed sea $\tilde{\Omega} = 0.83$ as a function of wind speed $U_{10}$. For low wind speeds $U_{10} < 5$ m/s, the stress at the surface is dominated by the viscous drag, so momentum is transferred directly from the air flow to the water flow. This is in agreement with observations, that the sea surface is aerodynamically smooth for wind speeds below $2 - 3$ m/s (Geernaert, 1990). Analysis of the field experiment of Snyder et al. (1981) (wind speed in the range 2 to 7 m/s) by Harris *et al.* (1994) suggests that the water surface is more likely to be transitional or even smooth, than rough for the conditions of the experiment. Our results, presented in figures 2 and 3 confirm the analysis of Harris at al. (1994), that for light winds, a significant part of the momentum is transferred by viscous stress.

With wind speed increasing, most of the stress goes through waves, supporting up to 95% of the total stress for high winds. In this regime, the roughness of the sea surface can be described in terms of the Charnock relation. Caudal (1993) has

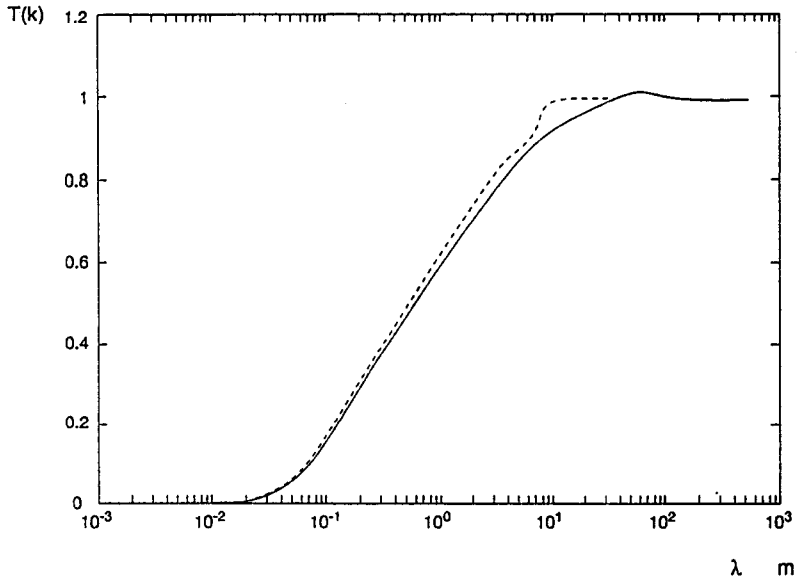


Fig. 4. Contribution of waves to the total wave-induced stress $\tau_0^w$, eq.(43). Solid line - $U_{10}/c_p = 0.83$, dashed - $U_{10}/c_p = 3$. Wind speed $U_{10} = 10$ m/s. Horizontal axis - wavelength $\lambda$ in m.

assumed that all the stress is supported by waves $u_*^2 = \tau_0^w$ for wind speeds higher than 7.5 m/s and also obtained the Charnock relation.

To assess which waves contribute most to the wave-induced stress, a function

$$T(k) = \frac{1}{\tau_0^w} \int_k^\infty M(k')\, \mathrm{d}k' \tag{43}$$

is plotted in Figure 4. Axis X corresponds to wavelength $\lambda(k) = 2\pi/k$. The inverse wave age is $\tilde{\Omega} = 0.83$ for a fully developed sea and $\tilde{\Omega} = 3$ for the young sea; the wind speed is 10 m/s. Function $T(k)$ shows an increase in wave momentum flux as longer waves are taken into account in the numerator of (43).

In both cases, 90% of the wave-induced stress is supported by waves shorter than 7 m. Less than 5% of this is supported by short gravity and gravity-capillary waves with length $\lambda \leq 5$ cm. This result confirms the finding of Caudal (1993), who showed that waves less than 3 cm contribute negligibly to the total stress. The gravity-capillary waves thus play a minor role in the transfer of momentum from wind to waves. The wave-induced stress to the gravity-capillary waves is quenched because the wave spectrum has a cut-off and because the wind input decreases and quenches the stress as waves become shorter.

In section 2.1.1. we have conditionally split the wave spectrum into two parts: "energy-containing" part $k < k_r$, which is wave-age dependent, and the "tail" $k > k_r$, which is wave-age independent. For the fully developed spectrum ($\lambda_p = 92$ m) the tail of the spectrum ($\lambda < \lambda_r = 7$ m) supports 90% of the total wave momentum flux. For a young sea ($\lambda_p = 7$ m), $\lambda_r = 1.4$ m, this amount reduces to

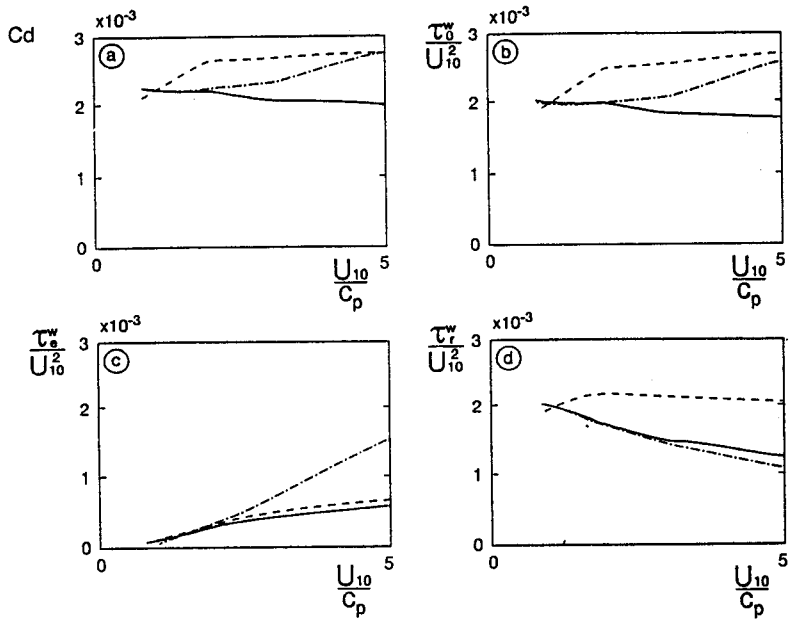


Fig. 5. a) Drag coefficient $C_d$ ; b) total wave-induced stress $\tau_0^w/U_{10}^2$; c) wave-induced stress to energy-containing waves $\tau_e^w/U_{10}^2$; d) wave-induced stress to the tail of a spectrum $\tau_r^w/U_{10}^2$ as a function of the inverse wave-age parameter $U_{10}/c_p$. Solid lines - Donelan-Pierson spectrum. Dashed-dotted - enhanced peak according to eq.(36). Dashed - enhanced tail according to $\Omega^{2/5}$. Wind speed $U_{10} = 15$ m/s.

75 %. For a young sea, the wave-age dependence of the energy-containing part of the spectrum becomes important in determining the drag coefficient, as it enters the range of wavelength $0.05 < \lambda < 7$ m which extracts momentum from the air.

Assuming that the Donelan and Pierson (1987) spectral form of the tail is valid for developing seas as well as for fully developed sea, no dependence of the drag coefficient on wave age for the given wind speed is found, Figure 5a. This fact is explained by Figure 5 b-d, where parts of the wave-induced stress going to the energy-containing part $k < k_r$ of the spectrum $\tau_e^w$, to the tail $k \geq k_r$ of the spectrum $\tau_r^w$, and the total stress $\tau_0^w = \tau_e^w + \tau_r^w$ are plotted.

While with increase of the inverse wave-age parameter $\tilde{\Omega}$, the stress $\tau_e^w$ increases due to the fact that (23) is wave-age dependent, the stress to the tail of the spectrum $\tau_r^w$ drops. Why this happens becomes clear from Figure 4. As the peak of the spectrum moves to higher wave numbers with increase of the inverse wave-age parameter, so does the patching wave number $k_r$ due to (35). Shorter and shorter waves then contribute to $\tau_r^w$. As the tail of the spectrum (33) is wave-age independent, the stress $\tau_r^w$ drops.

When the high wave-number part of the wave spectrum is allowed to be weakly wave-age dependent, e.g., as $\tilde{\Omega}^{2/5}$, the drag coefficient is found to increase about

30% for young seas $\tilde{\Omega} = 2 - 3$, Figure 5a. The stress to the tail of the spectrum $\tau_r^w$ now increases (Figure 5d) with inverse wave age and so does the total wave-induced stress and the surface drag.

When for the energy-containing part of the wave spectrum the dependence $\Omega^{3/2}$ is adopted due to (36), which is stronger than spectrum (23), the drag coefficient is found to increase about 10% for young seas $\tilde{\Omega} = 2 - 3$ and about 30% for a very young sea $\tilde{\Omega} = 5$, Figure 5a. The stress $\tau_e^w$ (Figure 5c) now compensates for the decrease in the $\tau_r^w$ stress (Figure 5d) and the wave-induced stress is wave-age dependent.

To summarize: if the high wave-number part of a wave spectrum (waves shorter than 7 m, or $k > 10k_p^0$) is sufficiently wave-age dependent due to the energy containing part or the high wave-number tail, the sea drag is also wave-age dependent.

Though there is some experimental evidence (see Section 2.1.1), that the high wave-number part of the wave spectrum is wave-age independent and that the energy-containing part has $\sim \tilde{\Omega}^{0.55}$ dependence on wave age, the actual form of wave spectra is not well established.

Here we want to leave open the issue of the actual dependence of the sea drag on the sea state. The proposed model of the WBL connects the sea drag mainly to the actual form of a wave spectrum. It is explained how the wave spectral form influences the formation of the sea drag. In this way, the model can be used to establish the actual form of a wave spectrum from a set of accurate drag coefficient measurements.

It is worthwhile to mention here that a wave spectrum in shallow water differs from a deep ocean spectrum due to interactions of waves with the bottom. Geernaert *et al.* (1986) pointed out that waves are steeper in shallow waters. The fact that the wave spectral form determines the wave-induced stress on the surface can influence the interpretations of combined near-shore and open ocean sea drag measurements (e.g. Donelan *et al.*, 1993).

The possibility of using the WBL model to simulate the field measurements of the HEXOS experiment (Smith *et al.*, 1992) is illustrated in Figure 6, where measured values of friction velocity are plotted against modelled values. The selected KNMI- HEXOS data set exactly corresponds to the one used in Smith et al. (1992), viz., the averaged concurrent sonic anemometer and pressure anemometer data for full runs with single-peaked spectra at the Dutch offshore research platform *Meetpost Noordwijk* (MPN). The range of measured wind speeds (recalculated to the height 10 m) is $11 - 20$ m/s and the range of the inverse wave- age parameter $U_{10}/c_p$ is $1 - 2$. The reported values of $c_p$ and $U_{10}$ are used to run the WBL model with the Donelan *et al.* (1985) and Donelan and Pierson (1987) wave spectral form. Modelled and experimental values of the friction velocity are then compared. The error bars correspond to an overall error of 10% in measured friction velocity. The modelled values of the friction velocity are found to be within the scatter of experimental data.

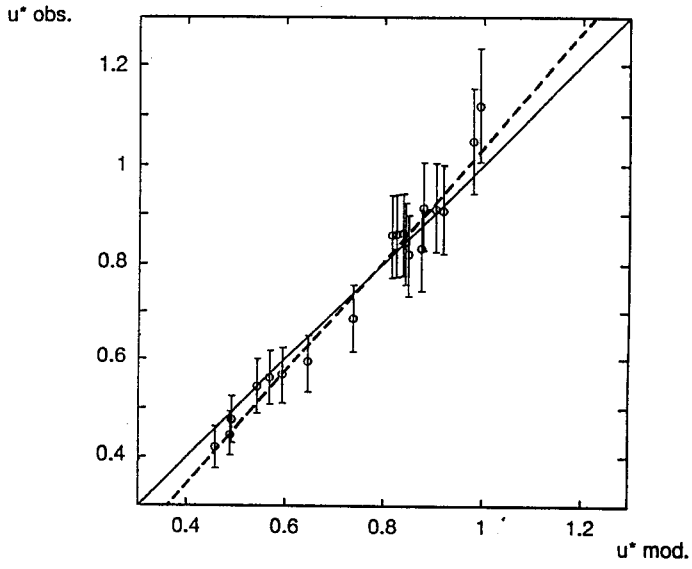


Fig. 6. HEXOS measured friction velocity against modelled friction velocity in m/s. Bars correspond to the overall error of 10% in measured friction velocity. Dashed line indicates the regression line.

However, the regression line with a slope of 1.16 and an intercept of -0.12 (correlation coefficient 0.98) shows that the model tends to underestimate values of the friction velocity at high wind speeds. A possible explanation is that waves at the MPN site may have been influenced at high wind speeds by the limited depth of 18 m (Maat *et al.*, 1991). It was already noticed in Smith et al. (1992) that the drag coefficient at the MPN site increases faster with wind than over the open ocean, but is similar to that at other sites with similar depth. The combined result for the MPN drag coefficient is approximated by their Equation 11. The measured friction velocity of the same data set plotted against the friction velocity calculated with Equation 11 of Smith *et al.* (1992) gives a regression line with a slope of 1.07 and an intercept of -0.05; the correlation coefficient is 0.98. The friction velocity calculated using their Equation 18 (our equation 7) for the roughness length gives a slightly better approximation to the selected data set (slope of regression line is 1.03, intercept is -0.03, the correlation coefficient is 0.98).

The form of wave spectra that we use in the model is for the condition of an open ocean and does not include a dependence on sea depth. A more precise comparison with the HEXOS data could have been made using in the model the one-dimensional wave spectra measured during HEXOS. However the buoy measurements of a wave spectrum are reliable in the frequency range of 0.06 - 0.60 Hz, which for the highest frequency corresponds to a wavelength of approximately 4 m. As we have found that most of the momentum is transferred to decimeter and meter waves, such a comparison would not be decisive before the form of wave spectra for higher frequency waves is measured and known.

## 4. Two-scale parameterization of the WBL

The two-scale parameterization of the WBL was suggested by Chalikov and Makin (1991) for energy-containing waves. Here it is extended for the full wave spectrum.

The step function approximation of the vertical distribution of the wave-induced stress:

$$\tau^w(z) = \tau_0^w \mathrm{He}(z_w - z) \tag{44}$$

(He($y$) is a Heaviside function, He = 1 at $y \geq 0$ and He = 0 at $y < 0$)) follows from exponential decay of the wave-induced stress with height (17). The characteristic decay height of the wave-induced stress is then:

$$z_w^{-1} = \frac{1}{\tau_0^w} \int_0^\infty 2kM(k)\,\mathrm{d}k. \tag{45}$$

From (9), (16), (12) and (44)

$$l\frac{\mathrm{d}u}{\mathrm{d}z} = (u_*^2 - \tau_0^w \mathrm{He}(z_w - z))^{1/2}, \tag{46}$$

an explicit solution for the velocity profile can be obtained:

$$u(z) = \frac{u_*^l}{\kappa} \ln \frac{z}{z_0}, \qquad z < z_w \tag{47}$$

and

$$u(z) = \frac{u_*}{\kappa} \ln \frac{z}{z_w} + \frac{u_*^l}{\kappa} \ln \frac{z_w}{z_0}, \qquad z \geq z_w. \tag{48}$$

From (48) and the upper boundary condition (19), the resistance law of the WBL is obtained:

$$r_1 u_* + r_2 (u_*^2 - \tau_0^w)^{1/2} = U_{10}, \tag{49}$$

where

$$r_1 = \frac{1}{\kappa} \ln \frac{h}{z_w}, \qquad r_2 = \frac{1}{\kappa} \ln \frac{z_w}{z_0}. \tag{50}$$

The drag coefficient of the sea surface $C_d = u_*^2/U_{10}^2$ follows from (49):

$$C_d^{1/2} = \frac{1}{r_1^2 - r_2^2} \left( r_1 - r_2 [1 - \frac{\tau_0^w}{U_{10}^2}(r_1^2 - r_2^2)]^{1/2} \right). \tag{51}$$

Equation (51) with (22) and (45) is solved by iterations as a function of the wind speed $U_{10}$. The wave- induced stress follows from (15), (16), where the wave spectrum and the growth wave parameter are updated due to the change of the wind

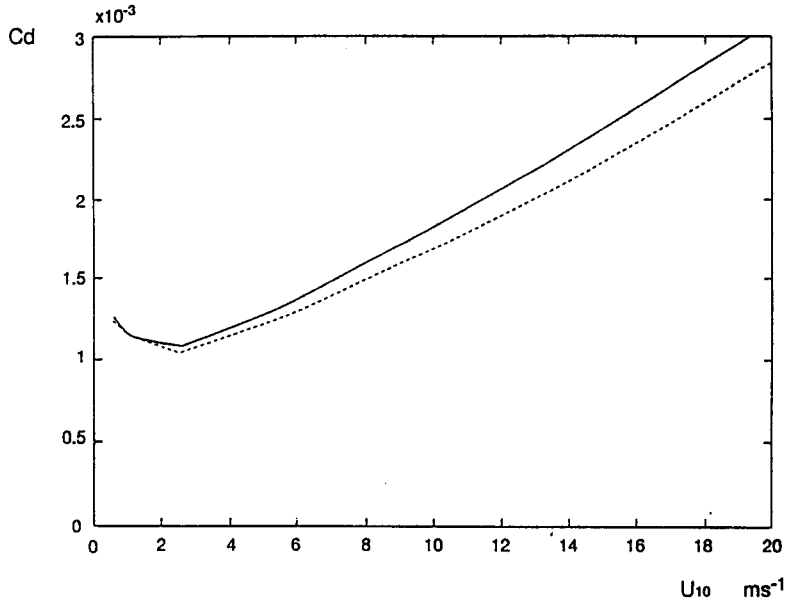


Fig. 7. Drag coefficient $C_d$ for fully developed sea as a function of wind speed $U_{10}$. Dashed line - full model of the WBL; solid - two-scale parameterization of the WBL.

profile (47), (48) and the drag $C_d$. The drag coefficient for a fully developed sea is compared with the previous WBL model calculation in Figure 7. The difference does not exceed 10%. That shows the validity of the two-scale parameterization of the WBL. The two-scale parameterization thus can be a useful tool in coupling atmospheric models with waves.

Equation (48) can be rewritten in the form

$$u(z) = \frac{u_*}{\kappa} \ln \frac{z}{z_e}. \tag{52}$$

The effective roughness parameter $z_e$ is defined sufficiently far above the waves as the constant in the logarithmic wind profile (52) and from (48)

$$z_e = z_0 \left( \frac{z_w}{z_0} \right)^{1-(1-\alpha_c)^{1/2}}, \tag{53}$$

where $\alpha_c = \tau_0^w / u_*^2$ is the coupling parameter.

The effective roughness is determined by the dynamical coupling of the wave-induced stress and the turbulent stress and strongly depends on the sea state. When the coupling parameter $\alpha_c$ is zero, which means there is no momentum flux due to waves, $z_e = z_0$, and the flow is aerodynamically smooth.

When $\alpha_c$ approaches 1, the coupling between waves and wind is strong, $z_e \to z_w$ and the sea surface is rough. As the coupling parameter is bounded by the condition $\alpha_c < 1$, the effective roughness parameter can never reach the height $z_w$. From

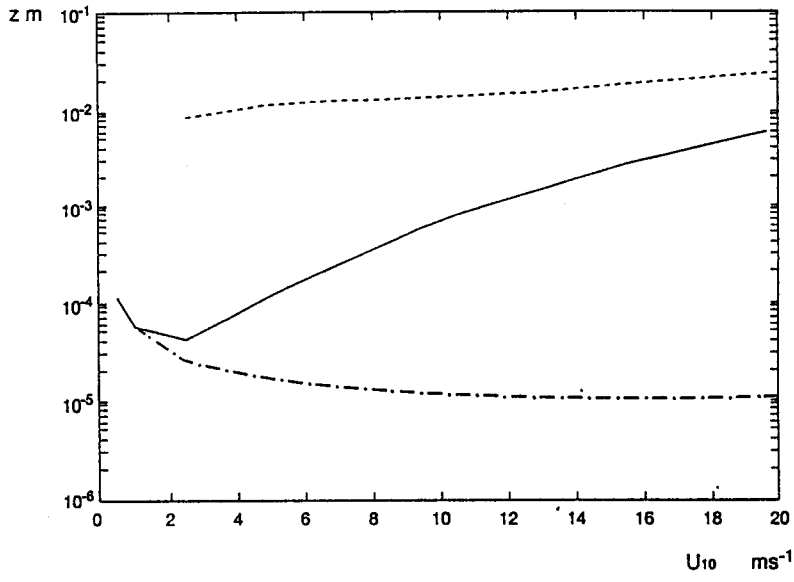


Fig. 8. Local roughness parameter $z_0$, eq.(22) (dashed-dotted line), effective roughness parameter, eq.(52) (solid line) and the decay height of the wave-induced stress $z_w$, eq.(45) (dashed line) in meters as a function of wind speed $U_{10}$ and for a fully developed sea.

(53) it follows that for rough flow the effective roughness $z_e$ is to a great extent determined by $z_w$. It means that to obtain a proper value of the effective roughness (the sea drag), the proper height dependence of the wave-induced stress, which determines this height (17), (45), should be chosen. With our choice of (17), we were able to reproduce the well known drag relations and accurate observations such as those of HEXOS.

Parameters $z_0$, $z_e$ and $z_w$ as a function of the wind speed $U_{10}$ are shown in Figure 8 for a fully developed sea. While $z_w$ increases slightly with wind, the effective roughness $z_e$ is sufficiently determined by the wind speed (see also figure 2 for the sea drag $C_d = \kappa^2 / \ln^2(10/z_e)$ ).

For high winds, the local roughness $z_0$ becomes virtually a constant, which according to (20) means that the local friction velocity becomes a constant, Figure 9. The increase of the wave-induced stress with wind is thus compensated by the increase of the bulk friction velocity $u_*$ at the top of the WBL. As the height $z_w$ is only a few centimeters, it is very difficult to estimate experimentally the actual value of the turbulent stress at the sea surface.

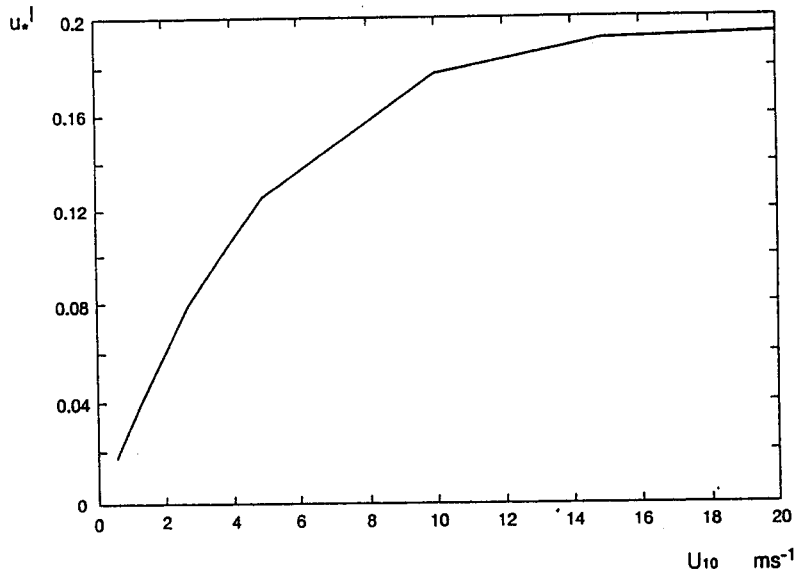


Fig. 9. Local friction velocity $u_*^l$, eq.(20) as a function of wind speed $U_{10}$ and for fully developed sea.

## 5. Discussion

The main objective of our paper is to develop a model of the WBL, which explains the formation of the sea drag for light to high winds for fully developed and developing seas. The drag of the sea surface is obtained as a result of the self-consistency between the wave spectral form, wind input, balance of the turbulent and wave-induced stress in the WBL and the boundary condition on the water surface.

By choosing the proper surface boundary condition, we were able to avoid the description of the background roughness parameter in terms of the Charnock-type relation, which is crucial in the former approaches of Janssen (1989), Chalikov and Makin (1991) and Chalikov and Belevich (1993). Instead, we have obtained the Charnock relation as a solution of the coupled system "waves-atmosphere" with a constant which is close to the experimentally observed one.

We show that the model is capable of simulating accurate field data of the HEXOS experiment within the 10% error in the measured friction velocity.

For high wind speeds ($U_{10} > 15$ m/s), most of the stress is supported by waves. For lower wind speeds, a considerable part of the stress is supported by viscous drag; for light winds, this permits aerodynamically smooth or transitional conditions of the sea surface.

It is shown that the gravity-capillary waves in the range of less than 5 cm are unimportant in supporting the sea drag. The cut-off in the momentum flux to those waves is a consequence of two mechanisms. First, the viscosity of the water

takes over the wind input and limits the growth of waves. Second, the growth-rate parameter quenches the wave growth, as the phase speed of capillary waves increases while the reference wind speed decreases with decrease of wavelength.

The problem is found to be sensitive to the wave spectral form in the full wave-number range, in particular the high wave-number part. If this latter part of the spectrum is wave-age independent, the sea drag appears to be virtually wave-age independent. If the high wave-number part depends on wave age, so also is the sea drag. That is consistent with earlier findings of Janssen (1989), Chalikov and Makin (1991) and Chalikov and Belevich (1993), who showed a strong dependence of the sea drag on wave age if the JONSWAP spectral form is adopted with an $\sim \tilde{\Omega}^{3/2}$ dependence on inverse wave-age parameter in the full wave-number range. When a weaker dependence $\sim \tilde{\Omega}^{2/3}$ on inverse wave age was adopted, the dependence of the drag coefficient on wave age diminished.

It appears that the form of the wave spectrum to a large extent determines the sea drag. There is contradictory evidence as to the actual form of the wave spectrum. Therefore, additional experiments are needed to settle this issue. More experimental evidence is needed to establish the relation of the drag coefficient on wave age.

## Acknowledgements

The authors wish to thank G. Komen, who provided strong scientific support for this study. Numerous discussions with him helped us shape our physical ideas. One of us wishes to thank G. Komen for providing the possibility to work in a very fruitful and stimulating atmosphere at KNMI. Our acknowledgements are for W. Oost for supplying experimental data over the HEXOS experiment. We also thank G. Burgers, W. Oost, J. Onvlee and A. Voorrips for stimulating discussions.

## References

Banner, M. L., Jones, I. S. F., and Trinder, J. C.: 1989, 'Wavenumber Spectra of Short Gravity Waves', *J. Fluid Mech.* **198**, 321–344.

Banner, M. L.: 1990, 'Equilibrium Spectra of Wind Waves', *J. Phys. Oceanogr.* **20**, 966–984.

Battjes, J. A., Zitman, T. J., and Holthuijsen, L. H.: 1987, 'A Reanalysis of the Spectra Observed in JONSWAP', *J. Phys. Oceanogr.* **17**, 1288–1295.

Burgers, G. and Makin, V.: 1993, 'Boundary-Layer Model Results for Wind-Sea Growth', *J. Phys. Oceanogr.* **23**, 372–385.

Caudal G.: 1993, 'Self-Consistency between Wind Stress, Wave Spectrum, and Wind-Induced Wave Growth for Fully Rough Air-Sea Interface', *J. Geophys. Res.* **98**, No. C12, 22743–22752.

Chalikov, D. and Belevich, M. Yu.: 1993, 'One-Dimensional Theory of the Wave Boundary Layer', *Boundary-Layer Meteorol.* **63**, 65–96.

Chalikov, D. and Makin, V.: 1991, 'Models of the Wave Boundary Layer', *Boundary-Layer Meteorol.* **56**, 83–99.

Charnock, H.: 1955, 'Wind Stress on a Water Surface', *Q.J.R. Meteorol. Soc.* **81**, 639–640.

Donelan, M. A.: 1982, 'The Dependence of the Aerodynamic Drag Coefficient on Wave Parameters', *Proc. First Int. Conf. on Meteorology and Air-Sea Interaction of the Coastal Zone*, The Hague, Amer. Meteor. Soc. 381–387.

Donelan, M. A., Hamilton, J., and Hui, W. H.: 1985, 'Directional Spectra of Wind Generated Waves', *Philos. Trans. R. Soc. London, Ser. A* **315**, 509–562.

Donelan, M. A. and Hui, W. H.: 1990, 'Mechanics of Ocean Surface Waves', *Surface Waves and Fluxes, Vol. 1*, G.L. Geernaert and W.J. Plant, Eds., Kluwer Academic, 336 pp.

Donelan, M. A. and Pierson, W. J.: 1987, 'Radar Scattering and Equilibrium Ranges in Wind-Generated Waves with Application to Scatterometry', *J. Geophys. Res.* **92**, No. C5, 4971–5029.

Donelan, M. A., Dobson, F. W., Smith S. D., and Anderson, R. J.: 1993, 'On the Dependence of Sea Surface Roughness on Wave Development', *J. Phys. Oceanogr.* **23**, 2143–2149.

Garratt, J. R.: 1977, 'Review of Drag Coefficients over Oceans and Continents', *Mon. Weather Rev.* **105**, 915–929.

Geernaert, G. L., Katsaros, K. B., and Richter, K.: 1986, 'Variation of the Drag Coefficient and its Dependence on Sea State', *J. Geophys. Res.* **91**, 1580–1584.

Geernaert, G. L.: 1990, 'Bulk Parameterizations for the Wind Stress and Heat Fluxes', in G. L. Greenaert and W. J. Plant (eds.), *Surface Waves and Fluxes, Vol. 1*, Kluwer Academic, 336 pp.

Harris, J. A., Belcher, S. E., and Street, R. L.: 1994, 'Linear Dynamics of Wind-Waves in Coupled Turbulent Air-Water Flow. Part 2. Numerical Model', *J. Fluid Mech.*, (accepted for publication).

Hasselmann, D. and Bösenberg J.: 1991, 'Field Measurements of Wave-Induced Pressure over Wind-Sea and Swell', *J. Fluid Mech.* **230**, 391–428.

Hsiao, S. V. and Shemdin, O. H.: 1983, 'Measurements of Wind Velocity and Pressure with a Wave Follower During MARSEN', *J. Geophys. Res.* **88**, C14, 9841–9849.

Jähne, B. and Riemer, K. S.: 1990, 'Two-Dimensional Wave Number Spectra of Small-Scale Water Surface Waves', *J. Geophys. Res.* **95**, 11531–11546.

Janssen, P. A. E. M.: 1989, 'Wave-Induced Stress and the Drag of Air Flow over Sea Waves', *J. Phys. Oceanogr.* **19**, 745–754.

Janssen, P. A. E. M.: 1991, 'Quasi-Linear Theory of Wind-Wave Generation Applied to Wave Forecasting', *J. Phys. Oceanogr.* **21**, 1631–1642.

Janssen, P. A. E. M.: 1992, 'Experimental Evidence of the Effect of Surface Waves on the Airflow', *J. Phys. Oceanogr.* **22**, 1600–1604.

JONSWAP Group (Hasselmann, K., Barnett, T. P., Bouws, E., Carlson, H., Cartwright, D. E., Enke, K., Ewing, J. A., Gienapp, H., Hasselmann, D. E., Kruseman, P., Meerburg, A., Müller, P., Olbers, D. J., Richter, K., Sell, W. and Walden, H.: 1971, 'Measurements of Wind-Wave Growth and Swell Decay During the Joint North Sea Wave Project (JONSWAP)', *Dtsch. Hydrogr. Z.*, **A8**(12), 1–95.

Kitaigorodskii, S. A.: 1970, *The physics of air-sea interaction*, Israel Program for Scientific Translations, Jerusalem, 1973.

Kitaigorodskii, S. A.: 1992, 'The Dissipation Subrange in Wind Wave Spectra', *Mat. Fys. Medd.* **42**(5), 3–24.

Larson, T. R. and Wright, J. W.: 1975, 'Wind-Generated Gravity-Capillary Waves: Laboratory Measurements of Temporal Growth Rates using Microwave Backscatter', *J. Fluid Mech.* **70**, 417–436.

Maat, N., Kraan, C., and Oost, W. A.: 1991, 'The Roughness of Wind Waves', *Boundary-Layer Meteorol.* **54**, 89–103.

Makin, V.: 1989, 'The Dynamics and Structure of the Boundary Layer Above Sea', Senior doctorate thesis, Inst. of Oceanology, Acad. of Sci. USSR, Moscow, 417 pp.

Makin, V.: 1990, 'Deviation of the Mean Wind Speed Profile Above Waves from the Logarithmic Distribution', *Izv. Atm. Oc. Phys.* **26**, 322–324.

Mastenbroek, C., Burgers, G., and Janssen, P. A. E. M.: 1993, 'The Dynamical Coupling of a Wave Model and a Storm surge Model through the Atmospheric Boundary Layer', *J. Phys. Oceanogr.* **23**, 1856–1866.

Monin, A. S. and Yaglom, A. M.: 1971, *Statistical Fluid Mechanics*, Vol. 1, Cambridge: MIT Press, 769 pp..

Phillips, O. M.: 1977, *Dynamics of the Upper Ocean*, 2nd ed. Cambridge University Press, 336 pp.

Plant, W. J.: 1982, 'A Relationship between Wind Stress and Wave Slope', *J. Geophys. Res.* **87**, 1961–1967.

Snyder, R. L., Dobson, F. W., Elliott J. A., and Long, R. B.: 1981, 'Array Measurements of Atmospheric Pressure Fluctuations Above Surface Gravity Waves', *J. Fluid Mech.* **102**, 1–59.

Stewart, R. W.: 1974, 'The Air-Sea Momentum Exchange', *Boundary-Layer Meteorol.* **6**, 151–167.

Smith, S. D., Anderson, R. J., Oost, W. A., Kraan, C., Maat, N., DeCosmo, J., Katsaros, K.B., Davidson, K. L., Bumke, K., Hasse, L., and Chadwick, H. M.: 1992, 'Sea Surface Wind Stress and Drag Coefficients: The HEXOS Results', *Boundary-Layer Meteorol.* **60**, 109–142.

Toba, Y., Iida, N., Kawamura, H., Ebuchi, N., and Jones, I. S. F.: 1990, 'Wave Dependence of Sea-Surface Wind Stress', *J. Phys. Oceanogr.* **20**, 705–721.

Wu, J.: 1980, 'Wind-Stress Coefficient Over Sea Surface Near Neutral Conditions – A Revisit', *J. Phys. Oceanogr.* **10**, 727–740.